Supporting Information

Supplementary Figures

Fig. S1.

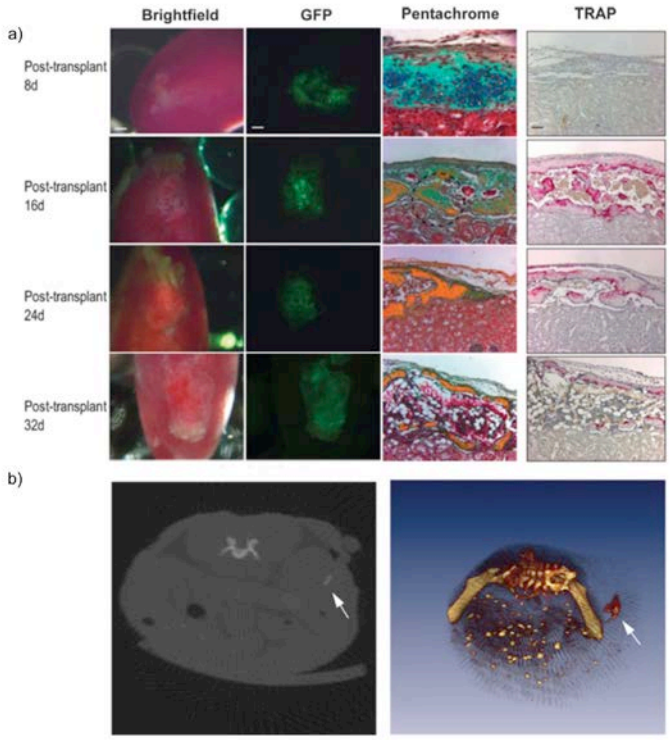

Fig. S1. <u>Endochondral ossification over time of GFP-labeled 14.5dpc CD45(-)Tie2(-)alphaV(+) limb progenitors transplanted under the renal capsule.</u> a) Ectopic bones forming at time points 8d-32d for each row; type of image or stain is indicated as the column heading. In (Movat's) pentachrome, bluish green indicates cartilage, yellow indicates osteoid. The tartrate resistant acid phosphatase (TRAP) stain shows osteoclast (red) infiltration. b) (Left) , MicroCT showing ossified graft (arrow) in kidney 32 days after transplantation. (Right) 3-D reconstruction of MicroCT scan from pelvic to lumbar region showing ectopic bone (arrow). (Scale bar in bright field and GFP images = 500 μm, in pentachrome and TRAP image = 100 μm)

Fig. S2

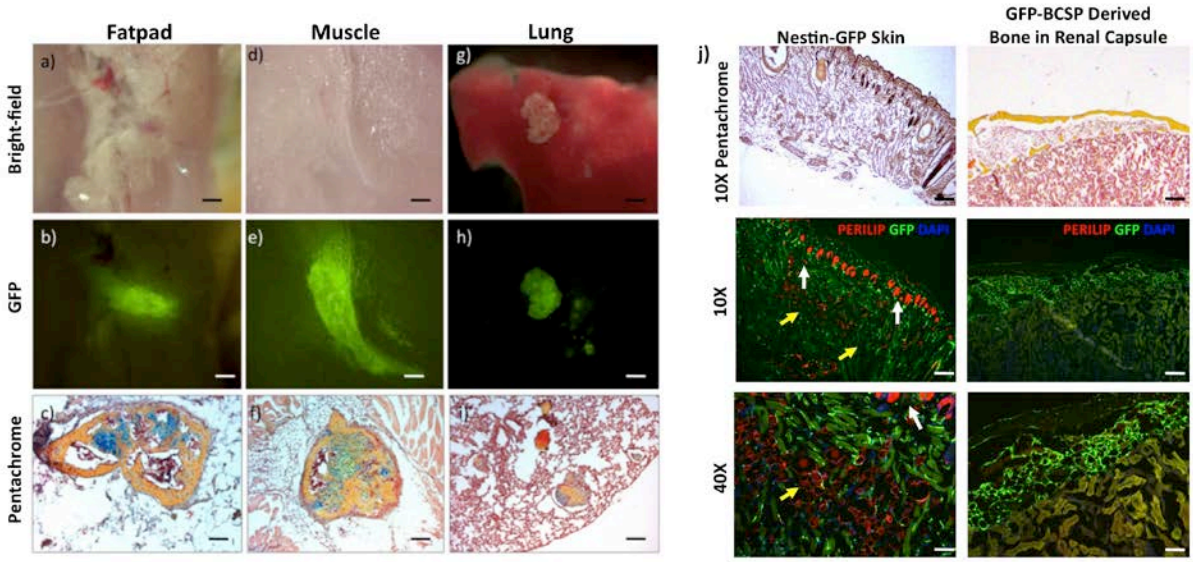

Fig. S2. **<u>BCSPs are committed to differentiate into skeletal tissues.</u>** GFP(+) extraskeletal bones formed 1 month after transplantation of GFP(+) BCSPs into subcutaneous fat (a-c), skeletal muscle (d-f), and lung (g-h). Top, middle, and bottom rows show brightfield, GFP, and pentachrome images of BCSP-derived bone. (j) BCSP progenitors do not contribute to significant adipogenesis *in vivo* . Top panels- Pentachrome images of skin from nestin-GFP mouse and GFP –labeled BCSP-derived bone in kidney capsule. Middle panels- immunodetection of perilipin (adipocyte marker) in skin versus lack of perilipin-positive cells in GFP-BCSP-derived bone. White arrows point to sebaceous glands. Yellow arrows point to adipocytes. Lower panels- Higher magnification of middle panels showing immunodetection of perilipin positive cells in skin and GFP-BCSP derived bone. White arrows point to sebaceous glands. Yellow arrows point to adipocytes. No perilipin positive cells were detectable in BCSP derived bone even at higher magnification. Scale bar = 10um Top Panels 100 μm lower panels)

Fig. S3.

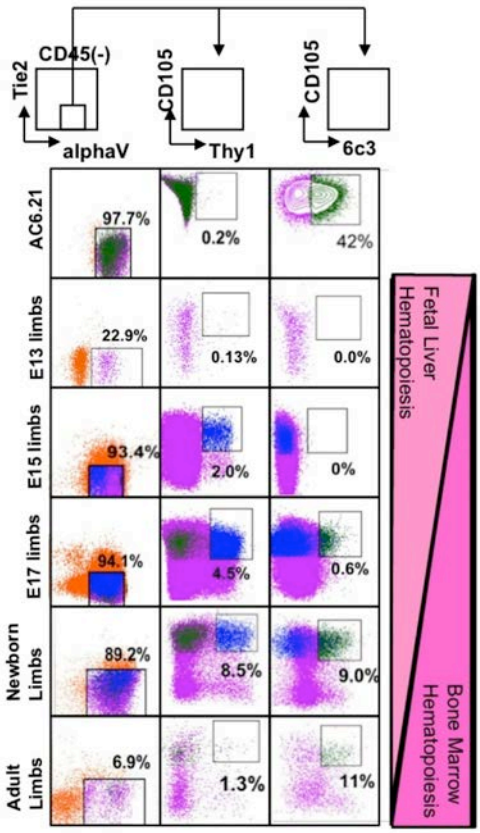

Fig. S3. **<u>Identification of 6C3 as a marker of skeletal progenitor-derived stromal cells.</u>** a) (Top panel) The gating scheme for FACS analysis of 6C3 expression in skeletal lineages. (Lower panels) FACS profiles of 6C3 expression in the AC6.21 stromal line and limb bone cells at distinct developmental stages. The percentage of parental population within the boxed population is inidicated. Limb bone cells were dissociated by collagenase digestion and stained without prior enrichment for skeletal lineage cells. 6C3 is coexpressed with CD105 in a subset of CD45(-)Tie2(-)alphaV(+) skeletal progenitors, expression of Thy1 and 6C3 appears to be mutually exclusive. 6C3 expression first appears at E17 dpc in fetal limb elements, when hematopoiesis migrates from the fetal liver to the bone marrow, as denoted by side bars.

Fig. S4.

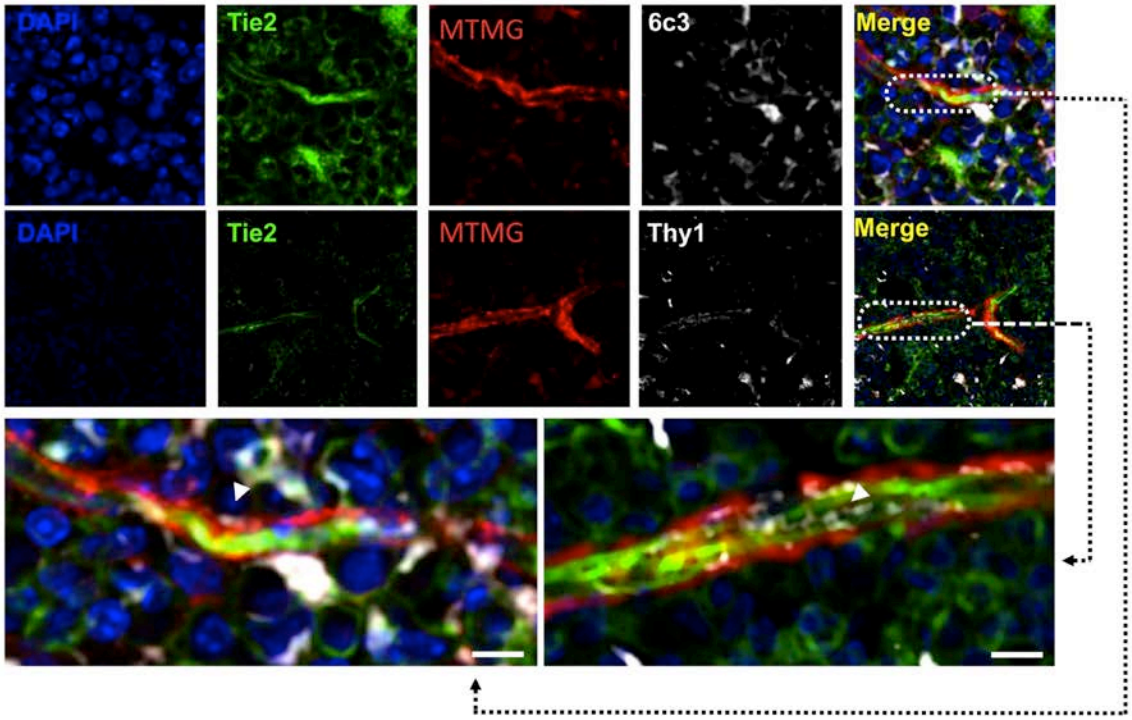

Fig. S4. <u>Stromal and perivascular localization of both Thy1+ and 6c3+ populations.</u>

Immunofluorescent staining of Tie2Cre transgenic mice crossed to mTmG (TomatoRed to GFP floxed-reporter mice) bone marrow showing that 6c3+ and Thy1+ cells (arrow) surround the Tie2+ vasculatures (green) and stromal compartment. Scale bar = 10 μm.

Fig. S5.

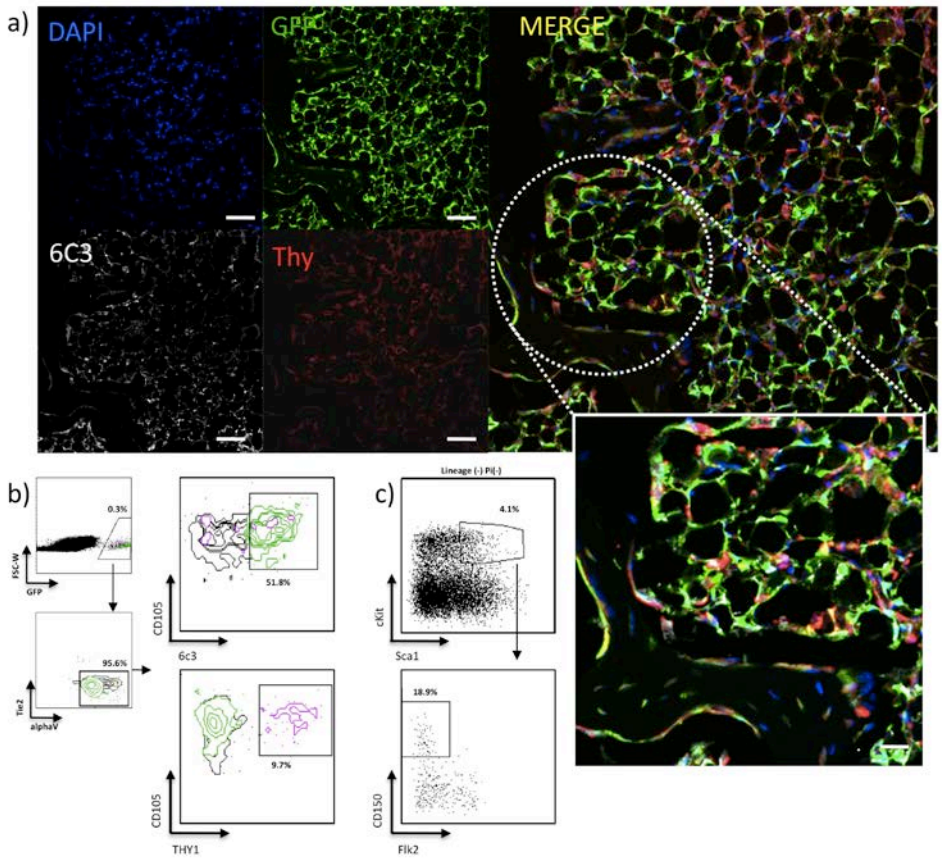

Fig. S5. **<u>Thy1 and 6C3 stroma are derived from BCSP.</u>** a) Immunofluorescent detection of 6C3 (+) and Thy(+) stroma in sections of GFP (+) ectopic bone formed in renal capsule one month after transplant of 100 thousand GFP(+)BCSP. b) FACS analysis of collagenase digested BCSP derived GFP (+) bone as described in (a) showing both Thy(+) and 6C3(+) stromal populations. c) FACS analysis of marrow in BCSP derived GFP (+) bone as described in (a) showing colonization by host-derived hematopoietic stem cells (HSC).

Fig. S6.

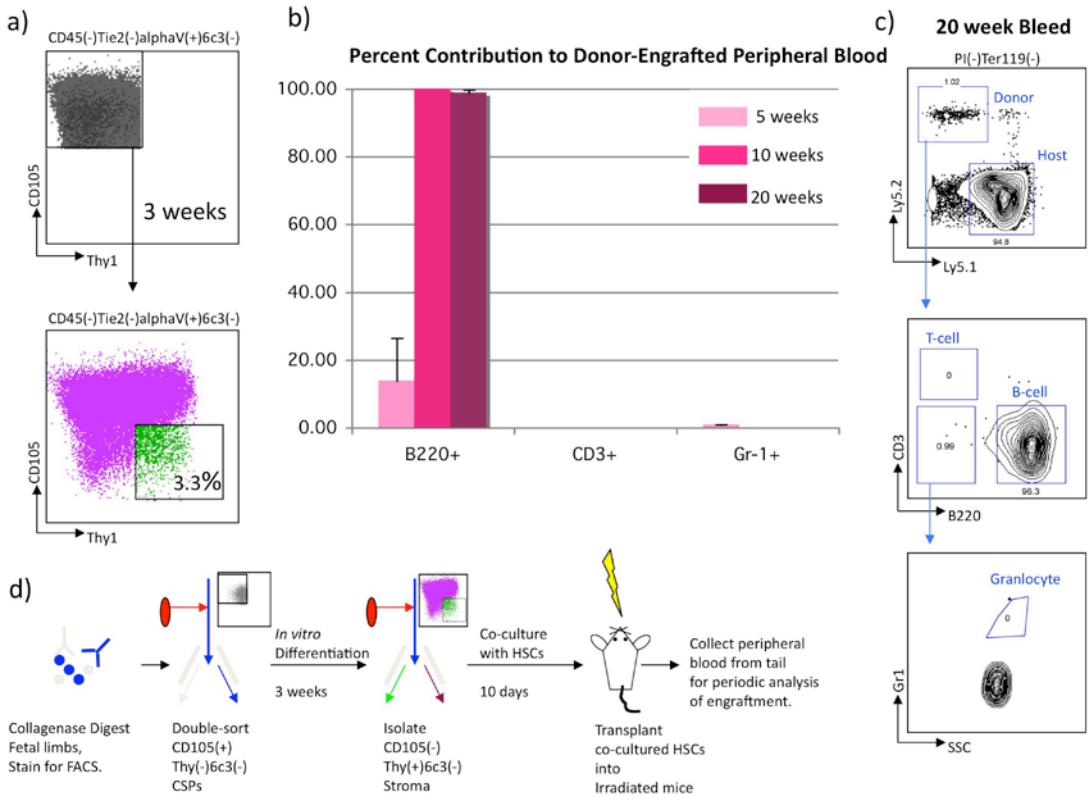

Fig. S6. <u>CD105(-)Thy(+)6C3(-) stroma derived from CD105(+)Thy(-)6C3(-) BCSPs drives specific HSC commitment to B-lymphpoiesis.</u> a) FACS profile of *in vitro* derivation of CD105(-)Thy(+)6C3(-) stroma from 200,000 CD45(-)Tie2(-)CD51(+)CD105(+)Thy(-)6C3(-) BCSP after three weeks in culture. Percent indicates fraction of CD105(-)Thy(+)6C3(-) population (boxed green) in parental population. After 21 days, CD105(-)Thy(+) cells were reisolated and plated with 250 freshly isolated Lin(-) Ckit(+)Sca1(+)CD34(-)Slamf1(+) HSCs and cultured for 10 days in serum free media containing SCF, TPO, IGF1 and FGF2 followed by transplant into lethally irradiated congenic recipients. b) Donor derived contribution to peripheral blood at 5, 10 and 20 weeks post-transplant. c) Representative FACS profile of peripheral blood in (b) after 20 weeks showing exclusive donor contribution to B lineages. d) Illustrated scheme of experiment.. * indicates $P<0.05$ by ANOVA, ** indicates $P<0.0001$ by ANOVA

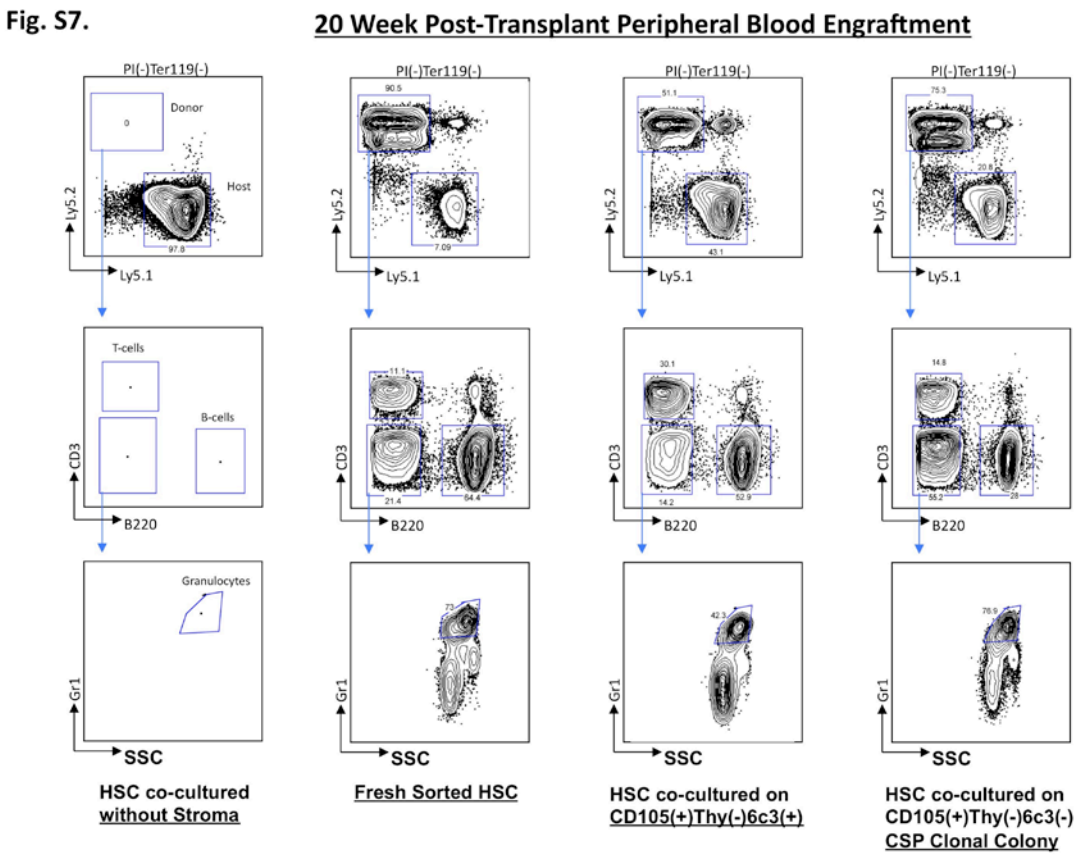

Fig. S7. **Long-term multilineage engraftment by HSCs cultured on skeletal progenitor-derived stroma.** Representative FACS profile of peripheral blood in lethally irradiated Ly5.1 congenic mice 20 weeks post-transplantion with Ly5.1 syngenic helper bone marrow and, a) 250 Ly5.2 HSCs cocultured without stroma, b) 20 fresh-sorted Ly5.2 HSCs, c) 250 Ly5.2 HSCs cocultured with CD105(+)Thy(-) 6C3(+) stroma derived from *in vitro* differentiation of CD105(+)Thy(-)6C3(-) skeletal progenitors, d) 400 Ly5.2 HSCs co-cultured with osteo-chondral-stromal colony derived from clone-sorted CD105(+)Thy(-)6C3(-) skeletal progenitors.

Fig. S8.

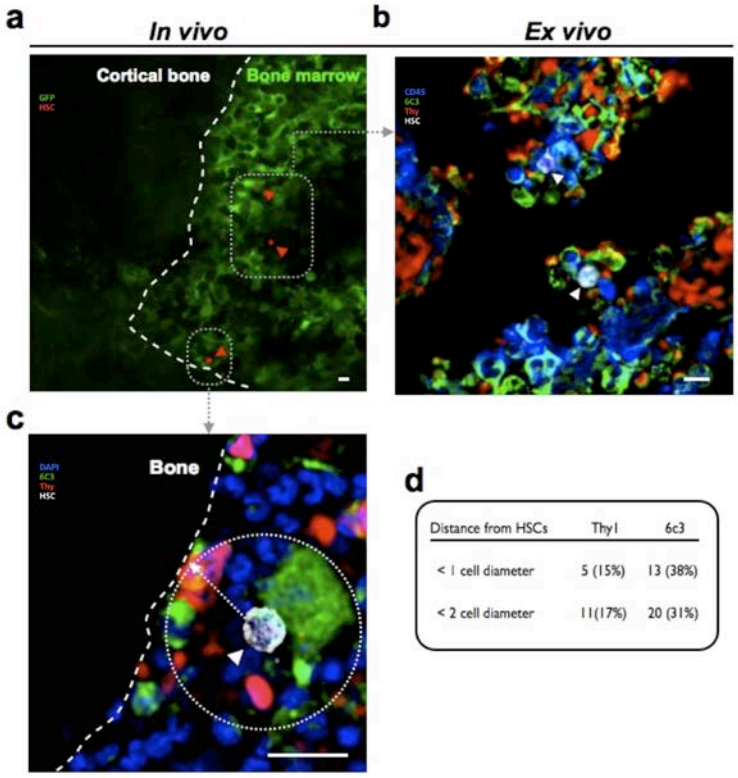

Fig. S8. **<u>Thy1+ and 6C3+ populations are in close contact with HSCs in the bone marrow.</u>**

Transplantation of RFP labeled HSCs (red arrows) following lethal irradiation showed endosteal localization of HSCs as shown by intravital imaging of the mouse tibia in vivo (a). These HSCs (white arrows) are in close contact with both Thy1+ (red) and 6c3+ (green) populations as demonstrated by immunofluorescence microscopy (b,c). Nearly all HSCs detected were localized within 1 cell distance from 6c3+ cell populations and 2 cell distance away from Thy1+ cells (c,d). In fact, nearly 40% of the cells within 1 cell radius surrounding the HSCs are 6C3+CD45- and 15% are Thy1+CD45-, with the rest being CD45+ hematopoietic lineages. For b), blue = CD45. For c), blue = DAPI. Scale bar = 20 μm.

Fig. S9.

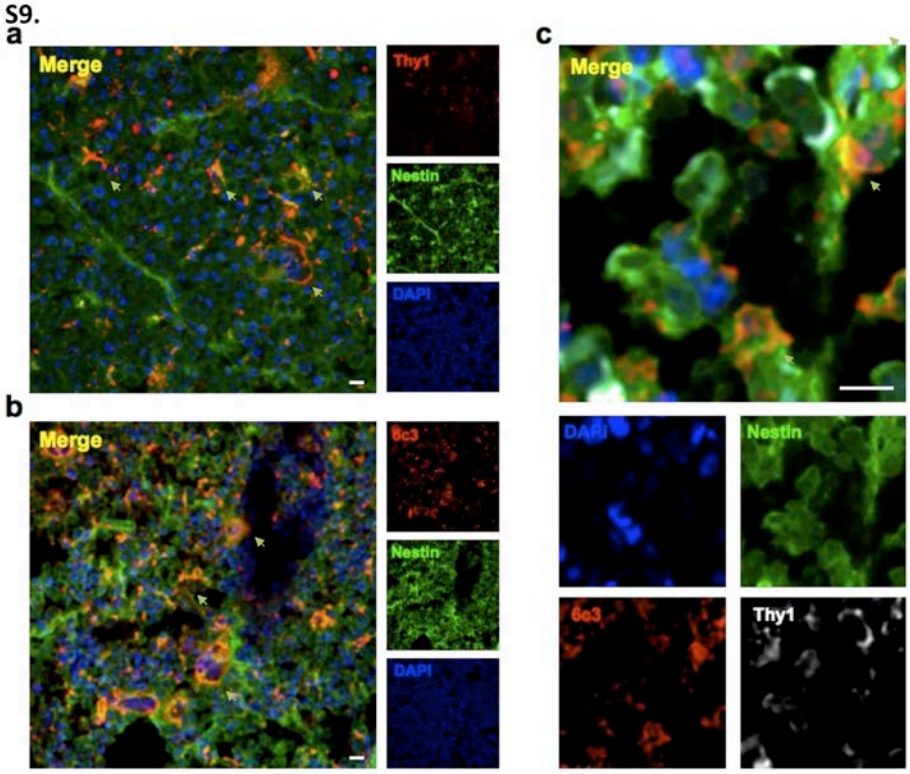

Fig. S9. **<u>Both Thy1+ and 6C3+ cell populations express nestin.</u>** Immunofluorescence stain for both Thy1 (a) and 6C3/BP-1 (b) of nestin-GFP bone marrow showed expression of Thy1 and 6C3 in nestin-GFP+ cells as demonstrated by co-localization of both fluorescence channels. Arrays point to nestin Co-staining for both Thy1 and 6C3/BP-1 (c) demonstrate that they are distinctive populations that express nestin as a common marker. Scale bar = 10 μm.

Fig. S10.

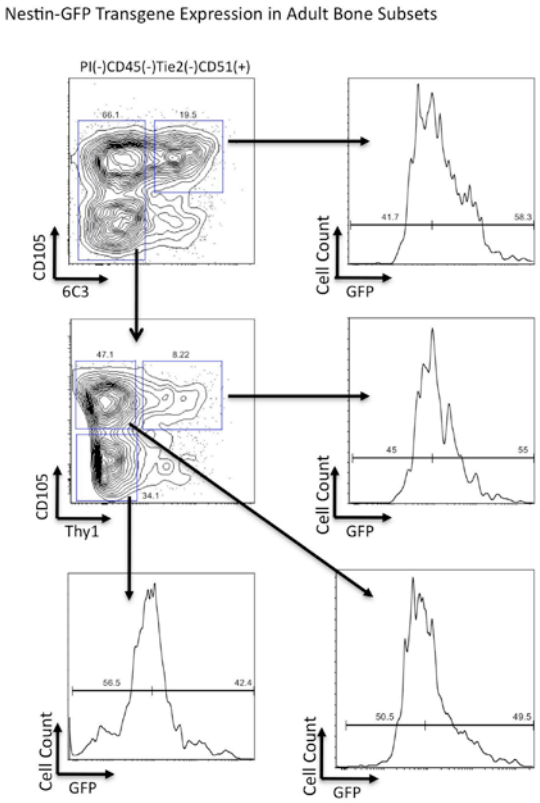

Fig. S10. <u>FACS Analysis of Nestin-GFP Expression in Bone Marrow Subsets</u>. Limbs from adult nestin-GFP transgenic mice were dissociated and stained with CD45, Tie2, CD51, CD105, Thy1, 6C3. Arrows indicate gating strategy. For each plot gates were determined based on both FMO (blue) and Isotype (red) controls. The numbers on the plot indicate the percentage of nestin positive cells in 10,000 collected events.

Fig. S11.

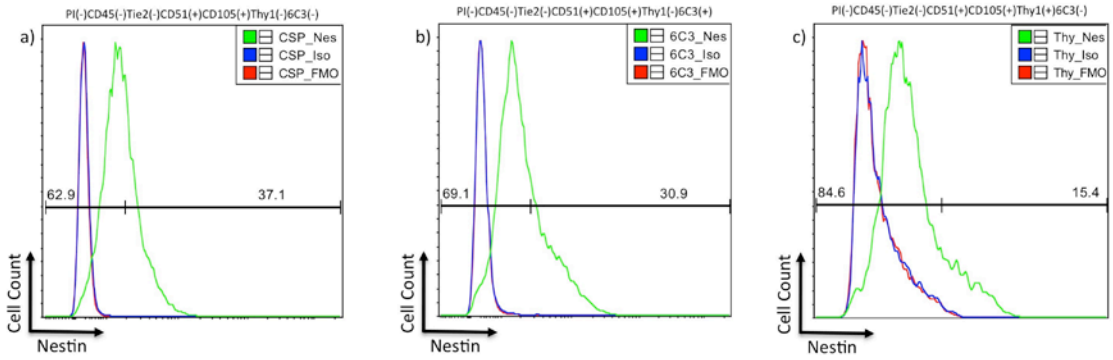

Fig. S11. <u>Intracellular FACS Analysis of Nestin Protein Expression in Bone Marrow Subsets</u>. Limbs from post-natal day 3 animals were dissociated and stained with CD45, Tie2, CD51, CD105, Thy1, 6C3 and nestin. For each plot gates were determined based on both FMO (blue) and Isotype (red) controls. The numbers on the plot indicate the percentage of nestin positive cells in 10,000 collected events.

Fig. S12.

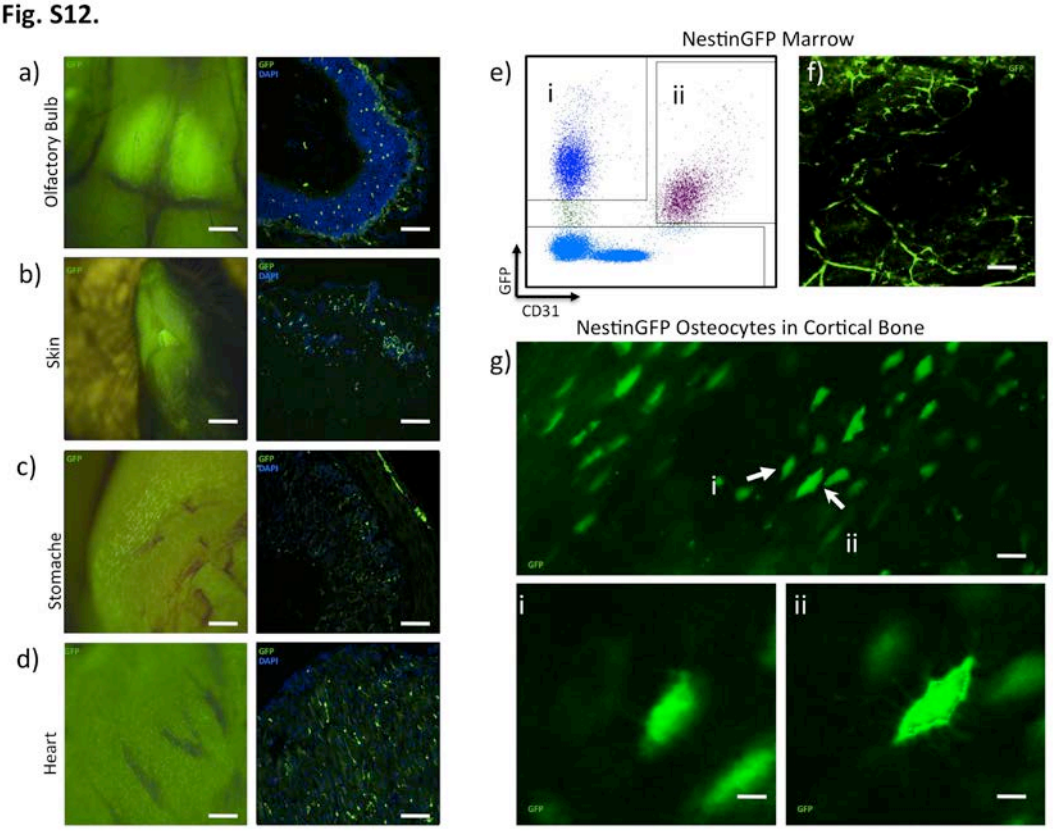

Fig. S12. **<u>Nestin expression is not specific to any one type of tissue or cells.</u>** Nestin postitive cells detected by Nestin-GFP reporter activity in the a) olfactory bulb, b) skin, c) stomache, and d)heart. Right panels shows nestin-GFP distribution in whole tissue. Left panel shows distribution of nestin-GFP in sectioned tissue co-stained with DAPI. e) FACS analysis of fresh-isolated bone marrow cells indicating that both CD31(-)non-endothelial cells(i), and CD31(+) endothelial cells in bone marrow express nestin-GFP. f) 2-photon microscopy of live bone marrow in nestin-GFP mice showing nestin-GFP (+) endothelium. g) 2-photon microscopy of live bone marrow in nestin-GFP mice showing nestin-GFP (+) mature osteocytes in cortical bone (i&ii). Lower panels shows osteocytes indicated by arrows in higher magnification. Nestin-GFP(+) processes of individual osteocytes projecting into canaliculi are visible.

Materials and Methods

Mice

C57BL/Ka-Thy1.1-CD45.1 (HZ), C57BL/Ka-Thy1.1-CD45.1 (BA), C57BL/Ka-Thy1.2-CD45.1 (Ly5.2) and C57BL/Ka-Thy1.2-CD45.1- actin GFP, and rosa26-mRFP (C57BL/6[B6]) strains were derived and maintained in our laboratory. Timed embryos from GFP transgenic B6 mice were used in most of the experiments in transplantation of fetal skeletal elements . Nestin-GFP mice were a kind gift of Grigori Enikolopov (43). Tie2/Cre and mT/mG (membrane-Tomato/membrane-Green) floxed reporter mice were obtained from Jackson Labs (52). All animals were maintained in Stanford University Laboratory Animal Facility in accordance with Stanford Animal Care and Use Committee and National Institutes of Health guidelines.

Isolation and transplantation of adult and fetal skeletal progenitors.

Fetal skeletal elements (humerus, radius, tibia, femur, and pelvis) were dissected from C57/BL6 BA strain fetuses and digested in collagenase with DNase at 37°C for 40 minutes under constant agitation. After collagenase treatment, undigested materials were gently triturated by repeated pipetting. Total dissociated cells were filtered through 40-mm nylon mesh, pelleted at 200*g* at 4°C, resuspended in staining media (2% fetal calf serum in PBS), blocked with rat IgG and stained with fluorochrome-conjugated antibodies against CD45, Tie2, α_V integrin, CD105, and Thy1.1 for purification by flow cytometry sorting. Sorted and unsorted skeletal progenitors were pelleted and resuspended in 2 ml of matrigel (regular), then injected underneath the renal capsule of 8-12 week old anesthetized mice.

For transplantation of adult limb bones (humerus, radius, tibia, femur, and pelvis) the same process was used as described in the previous paragraph, except the bones were gently crushed with a mortar and pestle after dissection and before digestion with collagenase.

Histological analysis of endochondral ossification.

Dissected specimens were fixed in 2% PFA at 4^{o}C overnight, then decalcified in 0.4M EDTA in PBS (pH 7.2) at 4°C for 2 weeks. Specimens were then processed for embedding in paraffin (by dehydration in alcohol or xylene) or OCT (by cryoprotection in sucrose) and sectioned. Representative sections were stained with either hematoxylin and eosin, Movat's modified pentachrome, Saffranin-O, or Alizarin red, depending on the experiments.

Immunofluorescence

Immunofluorescence on cryopreserved ectopic bone specimens were performed using an M.O.M. immunodetection kit from Vector Laboratories (CA) according to the manufacturer's instructions. Briefly, specimens were treated with a blocking reagent; probed with monoclonal antibody at 4^{o}C overnight; washed with PBS; probed with alexa-dye conjugated antibodies; washed; coverslipped; and imaged with a Leica DMI6000B inverted microscope system.

Immunofluorescence on tissue cultured cell specimens was performed with a method similar to that used for cryopreserved specimens. Briefly, cultured cells in 6-well to 96-

well culture plates were washed with PBS and fixed in 2% PFA at 4°C overnight. Specimens were treated with a blocking reagent, than probed with monoclonal antibody at 4°C overnight.

Paraformaldehyde fixed mouse bone marrow was labeled with anti-Thy1 (Santa Cruz) and biotinylated anti-6c3/BP-1 (eBiosciences) antibodies using a standard immunofluorescence staining protocol. After 3 rounds of washing with staining buffer, secondary antibodies were added. Specimens were next washed with PBS, probed with alexa-dye conjugated antibodies, washed, immersed in PBS, cover-slipped, and imaged with a the Zeiss LSM 510 Meta laser scanning confocal microscope. All images were analyzed using the NIH ImageJ software. Monoclonal antibody to mouse collagen II was purchased from NeoMarkers, monoclonal antibody to osteocalcin was purchased from Abcam. Alexa-dye conjugated secondary antibodies were purchased from Molecular Probes.

Cell culture.

Skeletal progenitors are cultured in vitro in MEM alpha medium with 20% FCS under low O_2 (2% atmospheric oxygen, 7.5% CO_2) conditions. Culture vessels were first coated with 0.1% gelatin. Cultured cells were lifted for analysis or passaging by incubating with M199 supplemented with 1mg/ml Collagenase II (Sigma)

HSC-stromal co-culture and transplant.

To establish stromal populations for HSC co-culture experiments, 200,000 CD105+Thy1-6C3-CD45-Tie2-alphaV+ BCSPs were fresh-sorted from dissociated bone and bone

marrow stroma of e15.5 dpc, e17.5 dpc, or newborn (post-natal day 0-3) mice, and plated on 0.1% gelatin coated 15-cm culture dish and supported with MEMalpha medium supplemented with 20%FCS and PenStrep (Invitrogen) antibiotic. Cells were cultured under low O_2 conditions (2% atmospheric oxygen, 7.5% CO_2). Two weeks after culture, cells were lifted by incubating with M199 medium supplemented with Collagenase II at 1mg/ml and then stained and FACs-sorted for indicated populations. A total of 5,000–10,000 cells of the indicated population were plated per well in 0.1 % gelatin-coated flat-bottom 96-well dishes. Populations were cultured for 1 week before HSC co-culture. For HSC co-culture, wells plated with stromal cells were first washed with StemPro (StemCell.com) stem cell culture medium to remove serum. Then 250 fresh sorted HSCs were added to the stromal cells and co-cultured in StemPro serum-free stem cell culture media supplemented with 10 ng/ml mouse recombinant steel factor (Peprotech), 5 ng/ml mouse recombinant Thrompopoietin (Peprotech), 20ng/ml basic fibroblast growth factor (R&D), and 25 ng/ml insulin growth factor (R&D). Culture medium was changed by removing and replacing half of it with fresh medium every other day for 10 days. On the 10th day, cells were removed for analysis and or transplanted to irradiated mice. For HSC transplants, the contents of each well corresponding to approximately 250 plated HSCs were combined with 300,000 unsorted host bone marrow cells as helper marrow and injected retro-orbitally into lethally irradiated (800 rad) congenic mice. Engraftment was assessed by FACS analysis of tail blood samples collected at 5, 10, and 15 week intervals for analysis of expression of congenic CD45.1 or CD45.2 and blood lineage–specific markers—i.e., B-cell (B220+CD3-), T-cell (CD3+B220-), and granulocyte (B220-CD3-Gr1hi-ssc(hi)) markers.

For HSC co-culture with clonal BCSP-derived colonies, multipotent colonies, as illustrated in Fig. 4d, were established by clone-sorting e15.5 BCSPs into 0.1% gelatin

coated flat-bottom 96-well plates. Colonies were allowed to grow for 3 weeks before HSC co-culture. Subsequently, 500 fresh-sorted HSCs were added to stromal colonies and co-cultured as described.

In vivo HSC tracking

For single HSC in vivo imaging and tracking, 15,000 RFP labeled HSCs were injected retro-orbitally into each GFP mouse and the bone marrow cavity were imaged within 5 hours of transplantation. The bone marrow window was prepared as previously described (1), and the mouse was immobilized onto the microscope stage using a custom-built platform to minimize micro-motion due to breathing and circulation. The mouse was kept alive on a heating pad and anesthesized via inhaled isofluorane. All imaging was done with a Prairie Ultima IV (Prarie Technologies, WI) upright *in vivo* two-photon microscope equipped with a 20X objective (N.A. 0.95). For the GFP channel, the emission filter used was 525±25 nm, and for RFP, the emission filter was 620±30 nm. All fluorophores were excited with a Ti:sapphire two-photon laser at an excitation wavelength of 900 nm (500 mW) (50).

MicroCT imaging.

Anesthetized or newly sacrificed animals were imaged on a GE Medical Systems eXplore RS MicroCT System.

Nestin Intracellular FACS.

Limbs from post-natal day 3 mice were isolated and dissociated as described above. Total dissociated cells were filtered through 40-um nylon mesh, pelleted at 200*g* at 4°C, resuspended in staining media (2% fetal calf serum in PBS), blocked with rat IgG, and stained with anti-mouse CD51 (clone RMV7) PE, anti-mouse CD45 (clone F30) PE-CY5, anti-mouse Ter119 PE-CY5, anti-mouse biotinylated CD105, anti-mouse 6C3, anti-mouse Tie2 (clone tek2) AlexaFluor680, and anti-mouse CD90.1 AlexaFluor 780. The secondary antibodies used were streptavidin PE-CY7 and goat anti-rat Quantum Dot 605. Following staining, propidium iodide was added and 100,000 cells from each of the specified populations was sorted on a BD FACS Aria II. The cells were then pelleted at 200*g* at 4°C and fixed in 2% parafomaldehyde for 1 hour at 4°C. Each population was permeabilized for 30 minutes with the detergent saponin and then stained with APC conjugated anti-mouse nestin (clone NESTIN) overnight at 4°C. A total of 10,000 events were then collected using a BD FACS Aria II.

Nestin-GFP FACS.

Femurs were harvested from 4-week old nestin-GFP transgenic mice. The marrow plug was flushed into collagenase buffer containing DNAse, using a 20-gauge needle. The remaining portion was minced in collagenase buffer using a razor blade. The marrow plug was placed in a 37°C incubator for 30 minutes. The minced cortical bone was

digested at 37°C for 45 minutes under constant agitation. The cells were then triturated and passed through a 40-μm mesh filter. Dissociated cells were pelleted at 200*g* at 4°C, resuspended in staining media (2% fetal calf serum in PBS), blocked with rat IgG, and stained with fluorochrome-conjugated antibodies against CD45, Tie2, a_V integrin, CD105, 6C3, and Thy1.1 for flow cytometric analysis.

Microarray analyses of BM Stromal progenitors.

We performed microarrays on BCSPs, Thy1+ cells, 6C3+ cells, and BLSPs. Each population was sorted in three independent sorts from limbs from 3- to 5-day-old male neonate. RNA was isolated with RNeasy Micro Kit (Qiagen) per manufacture's instructions. mRNA amplification was performed using a two-cycle target labeling system for 3' in vitro transcription, hybridized to a mouse genome 430 2.0 array, and scanned according to the manufacturer's protocol (Affymetrix). Background correction and signal normalization was performed using the standard multichip average algorithm (54-55).

References and Notes

1. Moore KA, Lemischka IR. (2006) Stem cells and their niches. Science. 311(5769):1880-5.

2. Ehninger A, Trumpp A. (2011) The bone marrow stem cell niche grows up: mesenchymal stem cells and macrophages move in. J Exp Med. 208(3):421-8.

3. Calvi LM, Adams GB, Weibrecht KW, Weber JM, Olson DP, Knight MC, Martin RP, Schipani E, Divieti P, Bringhurst FR, Milner LA, Kronenberg HM, Scadden DT. (2003) Osteoblastic cells regulate the haematopoietic stem cell niche. Nature. 425(6960):841-6.

4. Sacchetti B, Funari A, Michienzi S, Di Cesare S, Piersanti S, Saggio I, Tagliafico E, Ferrari S, Robey PG, Riminucci M, Bianco P. (2007) Self-renewing osteoprogenitors in bone marrow sinusoids can organize a hematopoietic microenvironment. Cell. 131(2):324-36.

5. Yamazaki S, Ema H, Karlsson G, Yamaguchi T, Miyoshi H, Shioda S, Taketo MM, Karlsson S, Iwama A, Nakauchi H. (2011) Nonmyelinating Schwann cells maintain hematopoietic stem cell hibernation in the bone marrow niche. Cell. 147(5):1146-58.

6. Zhang J, Niu C, Ye L, Huang H, He X, Tong WG, Ross J, Haug J, Johnson T, Feng JQ, Harris S, Wiedemann LM, Mishina Y, Li L. (2003) Identification of the haematopoietic stem cell niche and control of the niche size. Nature. 425(6960):836-41.

7. Wu JY, Scadden DT, Kronenberg HM. (2009) Role of the osteoblast lineage in the bone marrow hematopoietic niches. J Bone Miner Res. (5):759-64

8. Kopp HG, Hooper AT, Avecilla ST, Rafii S. (2009) Functional heterogeneity of the bone marrow vascular niche. Ann N Y Acad Sci. 1176:47-54.

9. Kiel MJ, Yilmaz OH, Iwashita T, Yilmaz OH, Terhorst C, Morrison SJ. (2005) SLAM family receptors distinguish hematopoietic stem and progenitor cells and reveal endothelial niches for stem cells. Cell.;121(7):1109-21.

10. Kiel MJ, Morrison SJ. (2008) Uncertainty in the niches that maintain haematopoietic stem cells.
Nat Rev Immunol. (4):290-301.

11. DiMascio L, Voermans C, Uqoezwa M, Duncan A, Lu D, Wu J, Sankar U, Reya T. (2007) J Immunol. Identification of adiponectin as a novel hemopoietic stem cell growth factor. 178(6):3511-20.

12. Naveiras O, Nardi V, Wenzel PL, Hauschka PV, Fahey F, Daley GQ. (2009) Bone-marrow adipocytes as negative regulators of the haematopoietic microenvironment. Nature. 460(7252):259-63

13. Méndez-Ferrer S, Michurina TV, Ferraro F, Mazloom AR, Macarthur BD, Lira SA, Scadden DT, Ma'ayan A, Enikolopov GN, Frenette PS. (2010) Mesenchymal and haematopoietic stem cells form a unique bone marrow niche. Nature. 466(7308):829-34.

14. Bhattacharya D, Czechowicz A, Ooi AG, Rossi DJ, Bryder D, Weissman IL. (2009) Niche recycling through division-independent egress of hematopoietic stem cells. J Exp Med. 206(12):2837-50.

15. Wright DE, Wagers AJ, Gulati AP, Johnson FL, Weissman IL. (2001) Physiological migration of hematopoietic stem and progenitor cells. Science. 294(5548):1933-6.

16. Chan CK, Chen CC, Luppen CA, Kim JB, DeBoer AT, Wei K, Helms JA, Kuo CJ, Kraft DL, Weissman IL. (2009) Endochondral ossification is required for haematopoietic stem-cell niche formation.
Nature. 457(7228):490-4.

17. Sweeney E, Campbell M, Watkins K, Hunter CA, Jacenko O. (2008) Altered endochondral ossification in collagen X mouse models leads to impaired immune responses. Dev Dyn. (10):2693-704.

18. Perin EC, Silva GV, Henry TD, Cabreira-Hansen MG, Moore WH, Coulter SA, Herlihy JP, Fernandes MR, Cheong BY, Flamm SD, Traverse JH, Zheng Y, Smith D, Shaw S, Westbrook L, Olson R, Patel D, Gahremanpour A, Canales J, Vaughn WK, Willerson JT.

(2011) A randomized study of transendocardial injection of autologous bone marrow mononuclear cells and cell function analysis in ischemic heart failure (FOCUS-HF). Am Heart J. 161(6):1078-87

19. Zeller R, López-Ríos J, Zuniga A. (2009) Vertebrate limb bud development: moving towards integrative analysis of organogenesis. Nat Rev Genet. (12):845-58.

20. Friedenstein AJ, Chailakhyan RK, Latsinik NV, Panasyuk AF, Keiliss-Borok IV. Stromal cells responsible for transferring the microenvironment of the hemopoietic tissues. Cloning in vitro and retransplantation in vivo. (1974) Transplantation. (4):331-40.

21. Pearse RV 2nd, Scherz PJ, Campbell JK, Tabin CJ. (2007) A cellular lineage analysis of the chick limb bud. Dev Biol. Oct 15;310(2):388-400.

22. Christensen JL, Wright DE, Wagers AJ, Weissman IL. (2004) Circulation and chemotaxis of fetal hematopoietic stem cells. PLoS Biol. (3):E75.

23. Morrison SJ, Hemmati HD, Wandycz AM, Weissman IL. (1995) The purification and characterization of fetal liver hematopoietic stem cells. Proc Natl Acad Sci U S A. 92(22):10302-6.

24. Muller-Sieburg CE, Whitlock CA, Weissman IL. (1986) Isolation of two early B lymphocyte progenitors from mouse marrow: a committed pre-pre-B cell and a clonogenic Thy-1-lo hematopoietic stem cell. Cell. 44(4):653-62.

25. Adkins B, Tidmarsh GF, Weissman IL. (1988) Normal thymic cortical epithelial cells developmentally regulate the expression of a B-lineage transformation-associated antigen. Immunogenetics. 27(3):180-6.

26. Whitlock CA, Tidmarsh GF, Muller-Sieburg C, Weissman IL. (1987) Bone marrow stromal cell lines with lymphopoietic activity express high levels of a pre-B neoplasia-associated molecule. Cell. 48(6):1009-21.

27. Spangrude, GJ, S Heimfeld and IL Weissman (1988). *Purification and characterization of mouse hematopoietic stem cells*. Science **241**(4861): 58-62.

28. Baum, CM, IL Weissman, AS Tsukamoto, AM Buckle and B Peault (1992). *Isolation of a candidate human hematopoietic stem-cell population*. Proc Natl Acad Sci U S A **89**(7): 2804-2808.

29. Shih CC, Hu MC, Hu J, Weng Y, Yazaki PJ, Medeiros J, Forman SJ. (2000) A secreted and LIF-mediated stromal cell-derived activity that promotes ex vivo expansion of human hematopoietic stem cells. Blood. 95(6):1957-66.

30. Szilvassy SJ, Weller KP, Lin W, Sharma AK, Ho AS, Tsukamoto A, Hoffman R, Leiby KR, Gearing DP. (1996) Leukemia inhibitory factor upregulates cytokine expression by a murine stromal cell line enabling the maintenance of highly enriched competitive repopulating stem cells. Blood. 87(11):4618-28.

31. Wu Q, Lahti JM, Air GM, Burrows PD, Cooper MD. (1990) Molecular cloning of the murine BP-1/6C3 antigen: a member of the zinc-dependent metallopeptidase family. Proc Natl Acad Sci U S A. 87(3):993-7.

32. Wu Q, Tidmarsh GF, Welch PA, Pierce JH, Weissman IL, Cooper MD. (1989) The early B lineage antigen BP-1 and the transformation-associated antigen 6C3 are on the same molecule. J Immunol.143(10):3303-8.

33. Sherwood PJ, Weissman IL. (1990) The growth factor IL-7 induces expression of a transformation-associated antigen in normal pre-B cells. Int Immunol.;2(5):399-406.

34. Zhang CC, Kaba M, Ge G, Xie K, Tong W, Hug C, Lodish HF. (2006) Angiopoietin-like proteins stimulate ex vivo expansion of hematopoietic stem cells. Nat Med. (2):240-5.

35. Weissman IL, Shizuru JA. (2008) The origins of the identification and isolation of hematopoietic stem cells, and their capability to induce donor-specific transplantation tolerance and treat autoimmune diseases.
Blood. 112(9):3543-53

36. Czechowicz A, Kraft D, Weissman IL, Bhattacharya D. (2007) Efficient transplantation via antibody-based clearance of hematopoietic stem cell niches. Science. 318(5854):1296-9.

37. Cao YA, Wagers AJ, Beilhack A, Dusich J, Bachmanvn MH, Negrin RS, Weissman IL, Contag CH. (2004) Shifting foci of hematopoiesis during reconstitution from single stem cells. Proc Natl Acad Sci U S A. 101(1):221-6.

38. Day K, Shefer G, Richardson JB, Enikolopov G, Yablonka-Reuveni Z. (2007) Nestin-GFP reporter expression defines the quiescent state of skeletal muscle satellite cells. Dev Biol. Apr 1;304(1):246-59.

39. Mignone JL, Roig-Lopez JL, Fedtsova N, Schones DE, Manganas LN, Maletic-Savatic M, Keyes WM, Mills AA, Gleiberman A, Zhang MQ, Enikolopov G. (2007) Neural potential of a stem cell population in the hair follicle. Cell Cycle. 6(17):2161-70.

40. Hoffman RM. (2011) Nestin-driven green fluorescent protein as an imaging marker for nascent blood vessels in mouse models of cancer. Methods Mol Biol. 689:183-204.

41. Uchugonova A, Duong J, Zhang N, König K, Hoffman RM. (2011) The bulge area is the origin of nestin-expressing pluripotent stem cells of the hair follicle. J Cell Biochem. 112(8):2046-50.

42. El-Helou V, Dupuis J, Proulx C, Drapeau J, Clement R, Gosselin H, Villeneuve L, Manganas L, Calderone A. (2005) Resident nestin+ neural-like cells and fibers are detected in normal and damaged rat myocardium. Hypertension. 46(5):1219-25.

43. Mignone JL, Kukekov V, Chiang AS, Steindler D, Enikolopov G. (2004) Neural stem and progenitor cells in nestin-GFP transgenic mice. J Comp Neurol. 469(3):311-24.

44. Sugiyama T, Kohara H, Noda M, Nagasawa T. (2006) Maintenance of the hematopoietic stem cell pool by CXCL12-CXCR4 chemokine signaling in bone marrow stromal cell niches. Immunity. Dec;25(6):977-88.

45. Ooi AG, Karsunky H, Majeti R, Butz S, Vestweber D, Ishida T, Quertermous T, Weissman IL, Forsberg EC. (2009) The adhesion molecule esam1 is a novel hematopoietic stem cell marker. Stem Cells. 27(3):653-61.

46. Yokota T, Oritani K, Butz S, Kokame K, Kincade PW, Miyata T, Vestweber D, Kanakura Y. (2009) The endothelial antigen ESAM marks primitive hematopoietic progenitors throughout life in mice. Blood. 113(13):2914-23.

47. Smith-Berdan S, Nguyen A, Hassanein D, Zimmer M, Ugarte F, Ciriza J, Li D, García-Ojeda ME, Hinck L, Forsberg EC. (2011) Robo4 cooperates with CXCR4 to specify hematopoietic stem cell localization to bone marrow niches. Cell Stem Cell. (1):72-83.

48. Ding L, Saunders TL, Enikolopov G, Morrison SJ. (2012) Endothelial and perivascular cells maintain haematopoietic stem cells. Nature. 481(7382):457-62.

49. Nakamura Y, Arai F, Iwasaki H, Hosokawa K, Kobayashi I, Gomei Y, Matsumoto Y, Yoshihara H, Suda T. (2010) Isolation and characterization of endosteal niche cell populations that regulate hematopoietic stem cells. Blood. 116(9):1422-32.

50. Wu JY, Purton LE, Rodda SJ, Chen M, Weinstein LS, McMahon AP, Scadden DT, Kronenberg HM. (2008)
Osteoblastic regulation of B lymphopoiesis is mediated by Gs{alpha}-dependent signaling pathways. Proc Natl Acad Sci U S A. Nov 4;105(44):16976-81.

51. Weissman IL. (1994) Developmental switches in the immune system.
Cell. 76(2):207-18.

52. Muzumdar MD, Tasic B, Miyamichi K, Li L, Luo L. (2007) A global double-fluorescent Cre reporter mouse.
Genesis. Sep;45(9):593-605.

53. Lo Celso C, Fleming HE, Wu JW, Zhao CX, Miake-Lye S, Fujisaki J, Côté D, Rowe DW, Lin CP, Scadden DT. (2009) Live-animal tracking of individual haematopoietic stem/progenitor cells in their niche.
Nature. 457(7225):92-6

54. Sahoo D, Seita J, Bhattacharya D, Inlay MA, Weissman IL, Plevritis SK, Dill DL. (2010) MiDReG: a method of mining developmentally regulated genes using Boolean implications. Proc Natl Acad Sci U S A. 107(13):5732-7.

55. Inlay MA, Bhattacharya D, Sahoo D, Serwold T, Seita J, Karsunky H, Plevritis SK, Dill DL, Weissman IL. (2009) Ly6d marks the earliest stage of B-cell specification and identifies the branchpoint between B-cell and T-cell development. Genes Dev. 23(20):2376-81.

56. Weissman IL, Baird S, Gardner RL, Papaioannou VE, Raschke W. (1977) Normal and neoplastic maturation of T-lineage lymphocytes. Cold Spring Harb Symp Quant Biol.;41 Pt 1:9-21.